

Article

Effects of Bio-Coal Briquette for Residential Combustion on Brown Carbon Emission Reduction

Juan Qi ^{1,2} and Jianjun Wu ^{2,*}

¹ School of Chemical Engineering and Technology, Xuzhou College of Industrial Technology, Xuzhou 221140, China; qij@mail.xzcit.cn

² National Engineering Research Center of Coal Preparation and Purification, School of Chemical Engineering and Technology, China University of Mining and Technology, Xuzhou 221116, China

* Correspondence: wujj@cumt.edu.cn

Abstract: Biomass burning is an important source of brown carbon (BrC) which poses high-risk threats to human health and the environment. In this study, bio-coal briquette (coal mixed with biomass), a promising solid fuel for residential combustion, is proven to be a clean fuel which can effectively reduce BrC emission. First of all, an orthogonal experiment with three factors and three levels on the physical property of bio-briquette was carried out to identify the optimal preparation conditions including the ratio of biomass to anthracite, particle size and molding pressure. Then a combustion experiment of the bio-coal briquetted was implemented in a simulated residential combustion system. BrC emission factors (EFs) were calculated based on the detected black carbon (BC) concentration by an aethalometer, and other optical characteristics for organic components of extract samplers, such as mass absorption efficiency (MAE) and absorption angstrom index (AAE), were also explored. Lastly, composition analysis of BrC by a gas chromatography (GC) tandem mass spectrometer (MS) and direct visible images by scanning electron microscopy (SEM) were investigated to provide more detail information on BrC EFs and property change. It was shown that bio-coal briquette had such low BrC EFs that 70–81% BrC was reduced in comparison with an interpolation value of 100% biomass and 100% coal. Furthermore, the composition of BrC from bio-coal briquette burning was different, which consisted of more substances with strong wavelength dependence. Consequently, although MAE declined by 60% at a 540 nm wavelength, the AAE value of bio-coal briquette only decreased slightly compared with interpolation values. To be more specific, tar balls, the main existing form of BrC, were distributed much more sparsely in the SEM image of bio-coal briquette. To sum up, a positive reduction effect on BrC was discovered in bio-coal briquette. It is evident that bio-coal briquette can serve as an alternative solid fuel for residential combustion, which is beneficial for both human health and the atmosphere.

Keywords: bio-coal briquette; BrC; combustion; residential solid fuel



Citation: Qi, J.; Wu, J. Effects of Bio-Coal Briquette for Residential Combustion on Brown Carbon Emission Reduction. *Processes* **2023**, *11*, 1834. <https://doi.org/10.3390/pr11061834>

Academic Editor: Albert Ratner

Received: 26 April 2023

Revised: 9 June 2023

Accepted: 15 June 2023

Published: 16 June 2023



Copyright: © 2023 by the authors. Licensee MDPI, Basel, Switzerland. This article is an open access article distributed under the terms and conditions of the Creative Commons Attribution (CC BY) license (<https://creativecommons.org/licenses/by/4.0/>).

1. Introduction

1.1. Research Motivation

In recent years, BrC has aroused widespread concern for its strong light absorption performance of ultraviolet (UV) and visible (Vis) light [1–3]. The absorption contribution of BrC at short wavelengths can reach 20–50% [4–6]. This indicates that it has an important impact on atmospheric radiation forcing. As a mixture containing multiple organic substances, some specific chemical species in BrC are the critical factors for absorbing and scattering light [7–9]. Further, a series of toxicants are produced by these chemical species. They endanger human health when breathed into the human respiratory system [10,11].

1.2. Research Advance

There have been many studies on the source and characteristics of BrC. The main sources of BrC are known to be the incomplete combustion of biomass and fossil fuel at low

temperatures [12]. The light absorption capacity of BrC from fossil fuel combustion sources is stronger than that generated from biomass combustion sources. Nevertheless, the BrC from fossil fuel source has a higher wavelength dependence, which is possibly due to the fact that it contains more highly aromatic and macromolecular organic compounds [13,14]. The enhanced light absorption partly results from two factors: intermolecular interactions between aromatic compounds with multiple hydroxyl, aldehyde or ketone groups, and the formation of complex derived from aromatic compounds with multiple hydroxyl groups and transition metals [15,16]. There are significant seasonal differences in the optical characteristics of BrC. MAE and absorption coefficient (Abs) are considerably higher in winter than in other seasons. It can be attributed to the fact that a large amount of heating fuel is consumed in winter and fossil fuel and biomass are the main heating combustion fuel [13]. AAE represents the spectral dependence of light absorption efficiency [17]. This leads to the greater AAEs of BrC with carbonaceous aerosols over 1 [18,19]. The existence of BrC in aerosols makes the MAE increase more strongly towards shorter wavelengths due to a larger AAE for BrC than for BC. Furthermore, the upgrade of modified combustion efficiency (MCE) reduces AAE [20,21]. Less efficient burning phases (smoldering; MCE < 0.9) produce more BrC compared with more efficient burning conditions (flaming; MCE > 0.9) [22]. Therefore, there is a positive correlation between AAEs and OC (organic carbon)/EC (element carbon) ratios. Further, the larger AAEs of crop residues is attributed to their higher OC/EC ratios compared with coals [22].

The light absorption characteristics of BrC are closely related to its composition. The MAE of different BrC fractions depends mainly on the chemical structure of chromophores (e.g., unsaturation degree, oxidation state and molecular weight) and the ratio of chromophores species to non-light-absorbing organics [23]. Based on previous research, the primary components of BrC include polycyclic aromatic hydrocarbons (PAHs), humic-like substances (HULIS), tarry materials from combustion, and bioaerosols [24–26]. These substances mostly contain highly conjugated aromatic rings, and have high molecular weights that are directly linked to polar functional groups such as oxygen and nitrogen [27]. Over 40% light absorption of BrC from biomass combustion is provided by nonpolar compounds [28]. The absorption of BrC can be dominated or contributed by a few major chromophores. For example, aromatic rings in macromolecular materials significantly increase the light absorption of BrC at short wavelengths [23]. The chromophore has become the main factor affecting the light absorption characteristics of BrC, and its light absorption ability is positively correlated with the molecular weight and unsaturated degree of the chromophore [29–31]. Absorbance and fluorescence intensity of methanol-soluble components of BrC are stronger than that of water-soluble components, possibly because some substances (such as PAH_s) are extractable in organic solvents, but are almost insoluble in water [32]. BrC is an important component of tar balls [33]. Fresh tar balls have light absorption characteristics similar to atmospheric BrC with higher absorption efficiency towards the UV wavelengths, and nonpolar tar aerosols contain predominantly high molecular weight unsubstituted and alkyl-substituted PAHs, while polar tar aerosols consist of a large amount of oxidized aromatic substances (e.g., methoxy-phenols, benzenediol) with higher O:C ratios and carbon oxidation states [34].

1.3. Research Contribution

In China, firewood and bulk coal are still the most popular fuels in vast rural areas. They are one of the major sources of BrC, and their combustion conditions and types affect BrC emissions and composition. In order to reduce environmental pollution, Chinese government has encouraged application of biomass briquette and coal briquette in residential combustion since 2014. Bio-coal briquettes, a mixture of biomass and coal, have been recommended as suitable alternative solid fuel because of their low pollutant emissions and high thermal efficiency [35,36]. During bio-coal briquette combustion, the drawbacks of biomass and coal complement each other; therefore, better combustible qualities can be achieved [37]. The irregular texture with numerous cracks and cavities in bio-coal briquette

is highly favorable for fuel combustion since oxidant reaches the core of the fuel with less resistant [38]. In addition, biomass that scatters in bio-coal briquette is burnt before coal and numerous pores are formed. Such a structure facilitates the transfer of mass and heat, reduces the formation of oxygen-depleted zones, and hence declines emissions of pollutants [35,36]. Therefore, there is tremendous significance for exploration of bio-coal briquette on BrC emissions based on the hazards and impacts mentioned above. To our knowledge, this is the first study to use bio-coal briquette for BrC reduction. It provides sufficient data and theoretical support for the popularization and application of bio-coal briquette, especially the bio-coal briquette made from universal biomass and coal resources in China.

1.4. Research Novelty

Little research on the effects of bio-coal briquette for residential combustion on BrC emission reduction is available. The BrC reduction effect of bio-coal briquette for residential combustion remains unclear, and the emission reduction mechanism of bio-coal briquette for it should be further clarified. Our aim is to fully clarify the emission mechanism and characteristics of BrC from bio-coal briquette. An orthogonal experiment was conducted to determine the optimum preparation process of bio-coal briquette. Then the combustion experiment of bio-coal briquette was implemented in a simulated residential combustion system. The results were compared with those of pure biomass briquette and anthracite chunk. In addition to BrC EFs, this study investigated optical property of bio-coal briquette. The influence of BrC's chemical species on its optical property was also explored.

2. Materials and Methods

2.1. Materials

Rice straw and corn straw collected from Xuzhou of Jiangsu province in China were selected to prepare bio-coal briquette in this study. They were dried and shredded to the length of 1 mm, 2 mm, and 3 mm, respectively. Jindong anthracite, shredded to 1 mm, 2 mm, and 3 mm in diameter, was chosen and mixed with these biomasses. Polyvinyl alcohol was used as binder.

2.2. Experimental Methods

2.2.1. Experimental Scheme

The experimental scheme of this study is shown as Figure 1.

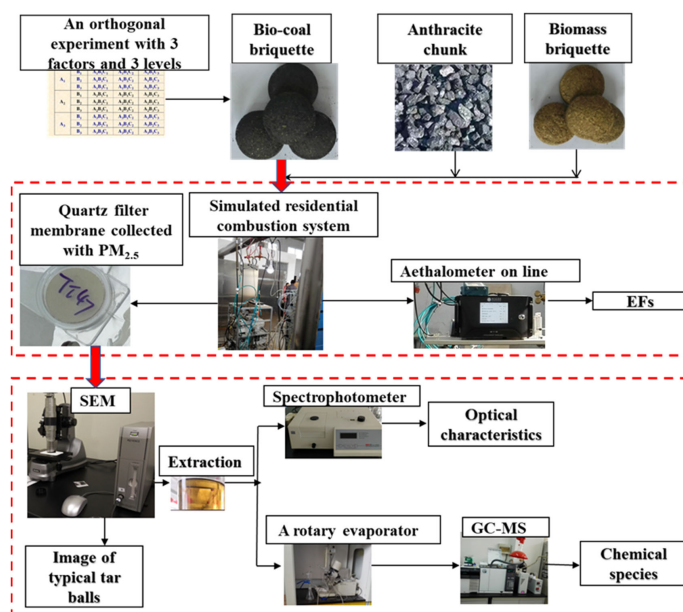


Figure 1. Experimental scheme for this study.

2.2.2. The Experimental System

A combustion experiment was implemented in a simulated residential combustion system (see Figure 2), including a combustion chamber and dilution sampling section. A typical residential stove and a kettle were adopted to simulate water boiling process. Generated flue gas was diluted in a pipe connected to flue gas hood above the stove. The power and stability of flue gas flow were provided by induced draft fan connected to the end of the pipeline. Sampling was conducted on the exhaust pipe (diameter of 22 cm) 4 meters away from the combustion chamber. An aethalometer (AE33, Magee Scientific, CA, USA) displaying 7 wavelengths ($\lambda = 950, 880, 660, 590, 520, 470, 370$ nm) was used to monitor the light absorption characteristics of BC in PM_{2.5} on line. Particle matter (PM) samples in two branches were gathered on quartz filter membrane (47 mm diameter, Pall Corp., Show Low, AZ, USA).

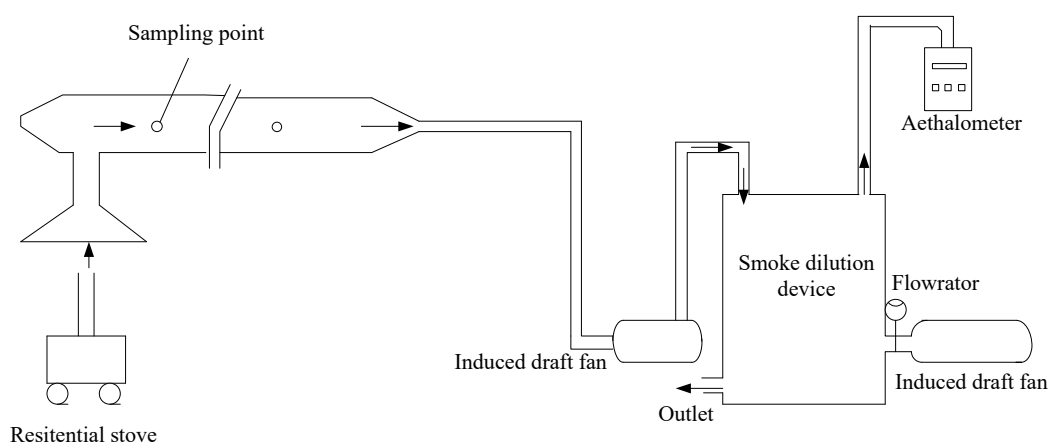


Figure 2. Simulated residential combustion system for the experiment test.

In order to obtain the optimum preparation process of bio-coal briquette, an orthogonal experiment with 3 factors and 3 levels (as shown in Table 1) was conducted. Three conditions including particle size, molding pressure, the mass ratio of biomass to anthracite were investigated. During the stirring of the mixture, 1 wt% polyvinyl alcohol diluted with water was added. As the key indicators of briquette, both compressive strength and shatter strength were measured to determine the optimum preparation process conditions.

Table 1. The orthogonal experimental scheme for bio-coal briquette process conditions.

No.	Particle Size (mm)	Molding Pressure (MPa)	Biomass/Anthracite (m/m)
1	≤ 1	15	1:9
2	≤ 2	25	1:4
3	≤ 3	35	3:7

2.2.3. Collected Sample Analysis

Before extraction, the quartz filter membrane collected with PM_{2.5} was analyzed by scanning electron microscopy (SEM; SU110, Hitachi Ltd., Tokyo, Japan) to monitor the morphology. Then the quartz filter membrane was extracted with dichloromethane with sonication for 30 min before it was kept at room temperature for 10 hours to allow the solution to reach equilibrium. After being sonicated for another 30 min, the extract was then filtered by syringe through a 50 mm diameter filter with a 0.45 μ m pore size to remove undissolved substance. Finally, the evaporated extract by a rotary evaporator was set to a constant volume of 1 mL before sample injection analysis. All extracts were analyzed by a GC (GC, Agilent 7890, Agilent Co., Palo Alto, CA, USA) tandem MS (Agilent 5975C, Agilent Co., Palo Alto, CA, USA). The GC capillary column was a HP-5 column

(30 m × 0.32 mm × 0.25 μm, Agilent Co., Palo Alto, CA, USA). The GC temperature was programmed from 50 °C (held for 2 min) to 316 °C at a rate of 3.5 °C/min, and then maintained for 5 min. Blank samples were analyzed with the same method, and their signals were deducted from those of the actual samples. MS conditions: electron ionization (EI): 70 eV, 230 °C. The selective ion monitoring (SIM) mode was adopted at a resolution of ≥10,000. The temperatures of injector and ion source were set at 280 °C and 260 °C, respectively. Ultrapure helium was used as the carrier gas under constant flow mode at a flow mode of 1.0 mL/min. After removing the blank, a peak was removed when the signal-to-noise ratio was less than 10 or the NIST library matching degree was less than 750.

Light absorption of these extracts without concentration were measured at 6 different wavelengths ($\lambda = 350, 420, 480, 540, 600$ and 700 nm) with a UV-vis double-beam spectrophotometer (UV-4802S, UNIC, Shanghai, China) at 1 nm intervals and 1 cm optical path. The BrC solution was placed in a 1 cm quartz cuvette. Pure dichloromethane was used as a blank reference for the solutions of BrC fraction. Blank samples and parallel samples were analyzed with the same method. Further, one-way ANOVA analysis was employed to confirm the validation of experimental results.

2.2.4. Calculation Method

1. EFs of BrC

The light absorption intensity increases exponentially with wavelength, and the change law conforms to the power law as Equation (1).

$$ATN = K \times \lambda^{-AAE} \quad (1)$$

where λ is the wavelength of the light; ATN is light absorption of BrC at wavelength of λ ; K is the constant of the mass concentration of the PM.

By deforming Equations (1) and (2), the following was obtained.

$$\ln(ATN) = -AAE \times \ln(\lambda) + \ln(K) \quad (2)$$

Fitting operations are performed on the ATN values measured by the 7-wavelength aethalometer at various wavelengths to obtain K and AAE . λ is an independent variable, and ATN is a dependent variable. Then the relationship between ATN_{SUM} and λ is established. ATN is varied on the λ . To let $AAE = 1$, the relationship between ATN_{SUM} and λ evolves into the relationship of ATN_{BC} and λ . By using the method of constant integral, the area of the two functions of ATN_{BC} and ATN_{SUM} are enclosed in wavelength 370–950 nm, and the difference area between the two is the ATN produced by BrC as Equation (3).

$$R_{BrC/BC} = \int (ATN_{SUM} - ATN_{BC})d\lambda / \int ATN_{BC}d\lambda \quad \lambda \in (370, 950) \quad (3)$$

where $R_{BrC/BC}$ is the concentration ratio of BrC to BC . By integrating the concentration of BC , the concentration of BrC can be estimated.

The BrC EFs were calculated as Equation (4)

$$EFs = \frac{Q_f \rho_s}{M_c} \int_{starttime}^{extinctiontime} R_{BrC/BC} C_s dt \quad (4)$$

where C_s (mg/m^3) is measured BC concentration by the aethalometer, ρ_s is the BC density, and Q_f is the gas flow rate in the tunnel.

2. Measurement of MAE and AAE

MAE and AAE are used to characterize the light absorption with the change in wavelength. Abs at wavelength of λ nm (Abs_λ) was calculated as Equation (5).

$$Abs_\lambda = (ATN_\lambda - ATN_{700}) \times \frac{V_1}{V_a \cdot l} \times \ln(10) \quad (5)$$

where V_1 (mL) stands for the volume of extractant added to each filter membrane sample, and V_a (L) represents the corresponding sampling volume; l (m) is the optical path length of the quartz dish of the ultraviolet spectrophotometer; ATN_{700} is used to deduct the baseline drift produced by instrument.

ATN_λ was estimated as Equation (6).

$$ATN_\lambda = -\log\left(\frac{I}{I_0}\right) = l \times \sum_i (c_i) \times \varepsilon_{i,\lambda} \quad (6)$$

where c_i (mol/L) is concentration of light-absorbing substances in solution, ε_i represents the proportional constant of each component, l (cm) stands for the length of optical path.

MAE at 365 nm (MAE_{365}) can be obtained by Abs at 365 nm as Equation (7).

$$MAE_{365} = \frac{Abs_{365}}{M} \quad (7)$$

where M represents the soluble organic quality concentration for tested sample.

The relationship between Abs and λ can be expressed as Equation (8), The AAE value can be obtained by linear fitting of $lg Abs$ and $lg \lambda$ at 350–600 nm.

$$Abs = K \cdot \lambda^{AAE} \quad (8)$$

where K is the constant of the PM mass concentration. λ stands for the wavelength of the light.

3. EFs and an interpolation value of 100% biomass and 100% coal

The chemical species EFs were calculated as Equation (9)

$$EFs = M_f \times F / M_c \quad (9)$$

where M_f is the collected mass of chemical species in $PM_{2.5}$, M_c is the mass of solid fuel, and F stands for the ratio of total flow rate in the dilution tunnel to the sampling flow rate.

The calculated mass-weighted average value (y), which was interpolated between the values for 100% biomass and 100% coal according to mass inclusion of biomass and coal, was calculated as Equation (10).

$$y = x_b \times b\% + x_c \times c\% \quad (10)$$

where x_b , and x_c are measured values of biomass briquettes and coal briquettes, respectively, $b\%$ and $c\%$ stand for proportion of biomass and coal.

3. Results

3.1. Analysis of the Results of Orthogonal Experiments

The orthogonal experimental results for bio-coal briquette mixed anthracite with rice straw or corn straw is presented in Tables S1–S6. The sequence of influence strength for bio-coal briquette quality was the mass ratio of biomass to anthracite > molding pressure > particle size. The optimal combination of these factors of this study was: the mass ratio of biomass to anthracite of 20 %, the molding pressure of 25 MPa, and the particle size of raw material not more than 1 mm. The following tested bio-coal briquette samples were prepared according to the optimum processing conditions.

3.2. Optical Characteristics

Figure 3 shows the BrC EFs of measured smoke from different fuel burning in $PM_{2.5}$. The BrC EFs of bio-coal briquette is 0.42 ± 0.11 and 0.33 ± 0.12 g/kg for corn straw-coal and rice straw-coal briquette. They are very close to that of anthracite (0.35 ± 0.31 g/kg). Pure biomass briquette presented BrC EFs of 5.57 ± 1.38 g/kg for corn straw-coal briquette and 7.40 ± 1.45 g/kg for rice straw-coal briquette, respectively.

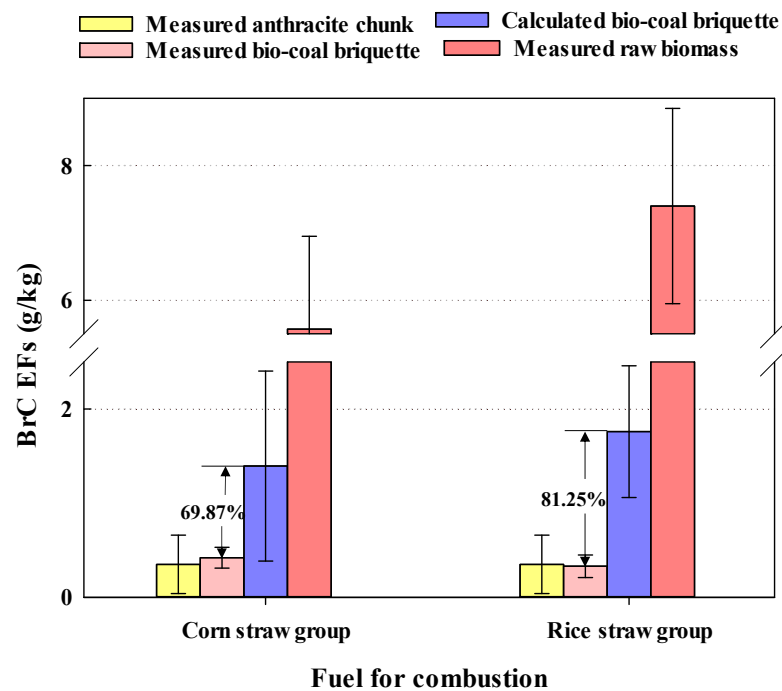


Figure 3. BrC EFs of combustion smoke from different fuel in $PM_{2.5}$ compared with calculated mass-weighted average ones.

There was a significant drop compared with the calculated mass-weighted average values. It is obvious that bio-coal briquette burning produced far less BrC. The reduction rate reached as high as 69.87% for corn straw-coal briquette and 81.25% for rice straw-coal briquette. More efficient burning phases reduces the production of BrC compared with more efficient burning conditions [22]. This trend is consistent with the $PM_{2.5}$ variation trend measured in the literature [35,36]. The addition of biomass into coal not only reduced $PM_{2.5}$, but also declined BrC emission. In addition, EFs of BrC obtained in this study are basically consistent with the data in the literature (see Table 2).

Table 2. BrC EFs of different solid fuel.

No.	Emission Source	EFs (g/kg)	Data Sources
1	Boio-coal briquette	0.33–0.42	This study
	Anthracite	0.35 ± 0.31	
	Biomass briquette	5.57–7.40	
2	Anthracite	1.08 ± 0.80	Sun et al. [39]
	Coal briquette	8.59 ± 2.70	
3	Peat	0.85	Stockwell et al. [40]
4	Firewood	7.50–16.00	Fan et al. [41]
5	Bituminous coal	2.10–3.10	Song et al. [42]
	Lignite	1.10–2.20	
6	Rice straw	2.50 ± 3.06	Sun et al. [43]
	Corn straw	0.45 ± 0.76	
	Biomass pellet	0.13 ± 0.06	

The MAE decrease proportion of bio-coal briquette is demonstrated in Figure 4. A similar decrease trend but with different values was presented by both MAE of corn straw-coal briquette and rice straw-coal briquette. Corn straw-coal briquette showed a more obvious reduction compared with rice straw-coal briquette at the same wavelength. Further, the

minimum value of $60.47 \pm 3.70\%$ reduction was achieved in rice straw-coal briquette at a 540 nm wavelength. The reduction in MAE also meant the drop of BrC EFs (as shown in Figure 3). MAE increased with the fraction of OC [44], the bio-coal briquette burning produced less OC. It could be attributed to the MCE improvement, resulting in complete OC combustion [35,36].

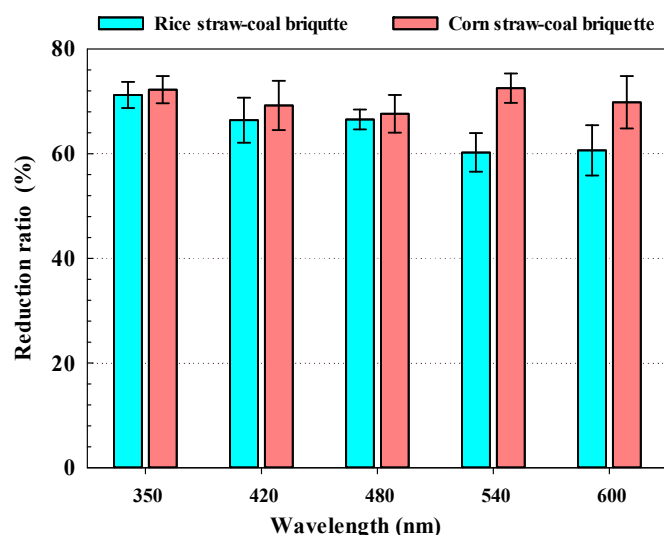


Figure 4. MAE reduction ratio of BrC from bio-coal briquette burning compared with calculated mass-weighted average ones.

AAE value was closely related to aerosols composition. There existed a positive correlation between AAEs and OC/EC ratios. The large AAEs for crop residues can be explained by their higher OC/EC ratios compared with coals [22]. The improvement of MCE of fuel significantly reduced the corresponding AAE [20,21]. Some studies have shown that AAE value is up to 9.5 for BrC [17], and BC is approximately 1 [15]. Although the AAE values of bio-coal briquette were slightly lower than the calculated mass-weighted average ones, no obvious change was discovered between them (see Figure 5). The reduction in BrC should account for the AAE decrease [18,19]. The phenomenon, however, was not consistent with the reduction in BrC EFs shown in Figure 3. The BrC from fossil fuel source had a higher wavelength dependence. The coal in bio-coal briquette produced more aromatic and macromolecular organic compounds than biomass [13,14].

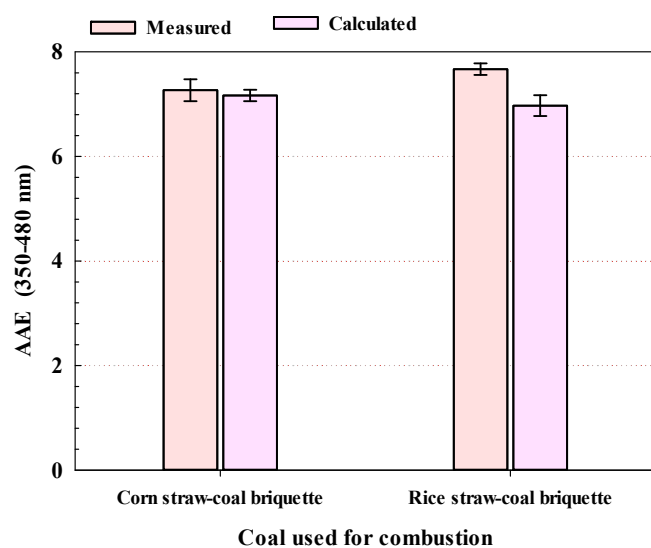


Figure 5. The AAE value from bio-coal briquette burning compared with calculated mass-weighted average ones.

The measured values of MEA and AAE were basically consistent with the data in the previous studies (see Table 3), which indicates the reliability of these data.

Table 3. Optical characteristics of BrC from different solid fuels.

No.	Emission Source	Wavelength (nm)	MAE (m ² /g)	AAE	Data Sources
1	Boio-coal briquette	350–480	0.10–0.36	7.31–7.70	This study
	Anthracite	350–480	1.33 ± 0.17	7.40 ± 0.23	
	Biomass briquette	350–480	1.17–1.28	5.30–6.23	
2	Corn straw	400–550		7–7.7	Li et al. [45]
3	Rice straw	300–400	1.37 ± 0.23	7.4–9.0	Park et al. [46]
4	Coal	365	1.5 ± 0.4	5.7 ± 0.2	Huang et al. [23]
5	Corn straw	375–625	2.10–3.10	1.5–4	Wang et al. [47]
	Rice straw	375–625	1.10–2.20	5.0 ± 0.1	
6	Bituminous coal	330–400	2.50 ± 3.06	7.7–11	Li et al. [48]
	Anthracite	330–400	0.13 ± 0.06	8.2–12	

3.3. Analysis of the Results of GC–MS Testing

Composition of particle samples from bio-coal briquette mixed with corn straw tested by GC–MS is shown in Figure 6. Compared with calculated mass-weighted values, as much as 30.22% EFs of total chemical species was reduced. In addition, chemical species proportion of bio-coal briquette were significantly different. In particular, alkenes EFs dropped by 85.60% and alkanes EFs sank by 81.74%. Therefore, phenols, esters and PAHs were the main components in these chemical emission from the bio-coal briquette burning. They were also the main wavelength dependence components [13,14]. All of them were actually less than calculated mass-weighted average ones in terms of EFs. The absorption of BrC could be dominated or contributed by these aromatic rings in macromolecular materials [23]. Intermolecular interactions between these PAHs caused the enhancement of light absorption [15,16].

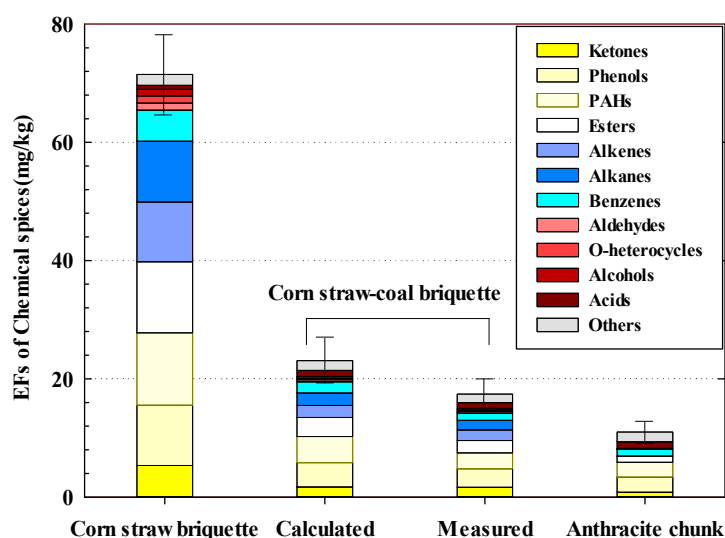


Figure 6. EFs of organic chemical species in PM_{2.5} emitted from different fuel combustion.

3.4. SEM Analysis

Figure 7 presents the SEM images of PM_{2.5} from corn straw-coal briquette. BrC existed in the form of tar balls. Tar balls significantly increased the direct radiation forcing in the near UV and UV light regions. Further, more than 95% of all particles emitted from biomass smoldering were tar balls [33,34]. The tar balls, each in the form of a spherical core with

bright outer shell, were distributed far more densely in the image of corn straw briquette. Further, other organic compounds were dark areas without a bright inclusion surrounded because they were largely electron transparent. A substantial reduction appeared in the image of corn straw-coal briquette, which had even less tar balls than anthracite chunk. Fresh tar balls had light absorption characteristics similar to atmospheric BrC with higher absorption efficiency towards the UV wavelengths [34].

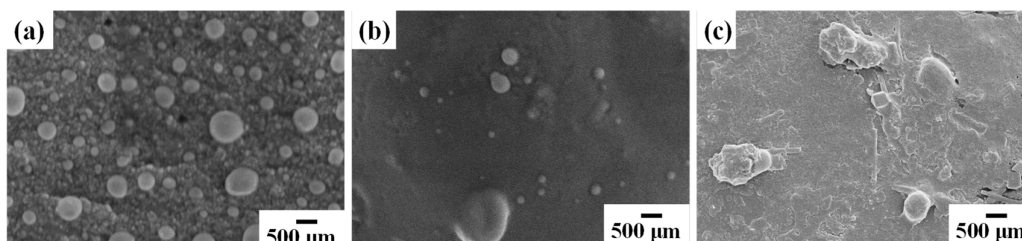


Figure 7. Scanning electron microscopy image of typical tar balls emitted from different fuel: (a) corn straw briquette, (b) corn straw-coal briquette, and (c) anthracite chunk.

4. Discussion

According to the trends in Figure 3, the AAE of bio-coal briquette should have presented a significantly reduction compared with the calculated mass-weighted average one. However, merely a little reduction was discovered. One of the most likely reasons was BrC composition change. It generated stronger wavelength dependence reflected on AAE. The effect of BrC EFs reduction on wavelength dependence was offset by some composition change in BrC produced in bio-coal briquette burning. Phenols, esters and PAHs, as the main components in BrC from the bio-coal briquette burning became the main factor for stronger light absorption characteristics of BrC [29–31].

The main chemical composition in PM_{2.5} sample of pure biomass briquette were alkanes, alkenes and PAHs. There was a marked difference in chemical composition of PM_{2.5} from anthracite burning, where more PAHs and phenols were discovered. They were characterized with higher wavelength dependence. The strong light absorption characteristics of BrC can be attributed to strong light-absorbing chromogenic groups, such as large molecules with aromatic and heteroatomic (O and N) groups [16,49,50]. The addition of biomass to anthracite effectively reduced the EFs of phenols and PAHs compared with calculated mass-weighted average ones, but their percentage increased somehow (see Figure 6). In short, although the total EFs of these chemical species decreased dramatically, relatively more wavelength dependent substances were left. This are probably the reasons for the BrC of bio-coal briquette with lower EFs but high stronger wavelength dependence. Although bio-coal briquette can improve MCE and reduce pollutants emission [35,36], the combustion of large molecules such as PAHs has not been fully resolved.

Biomass played a very important part in the BrC reduction. Compared with calculated mass-weighted average values, 69.87% for corn straw-coal briquette and 81.25% for rice straw briquette-coal was appreciably achieved by the synergistic effects. Synergistic effects between biomass and anthracite during bio-coal briquette combustion resulted in a considerable reduction in BrC emission. During bio-coal briquette combustion, oxidant reached the core of the fuel with less resistant because of the irregular texture with numerous cracks and cavities in it [38]. In addition, a large number of pores left after the combustion of biomass scattered in bio-coal briquette. This facilitated the transfer of mass and heat and reduced the formation of oxygen-depleted zones. MCE was improved and emissions of BrC declined accordingly [35,36].

5. Conclusions

In this study, bio-coal briquette was innovatively proposed for BrC reduction in residential solid fuel burning. To the author's knowledge, this is the first study to use bio-coal briquette for BrC reduction. Bio-coal briquette in this study was prepared according to

optimum process conditions obtained by a three-factor and three-level orthogonal test. BrC EFs, and MAE and AAE of BrC were investigated, and GC-MS and SEM were adopted for mechanism exploration. Some conclusions can be drawn as follows:

(1) According to the three-factor and three-level orthogonal test, the optimum processing conditions determined by shatter strength and compressive strength were: the ratio of biomass to anthracite is 20 %, the molding pressure 25 MPa, and the particle size of raw material not more than 1mm.

(2) Bio-coal briquette led to substantial BrC EFs reduction compared with calculated mass-weighted average ones. The corresponding MAE values decreased markedly at the wavelength of 350–600 nm as well. It is highly likely that higher MCE in bio-coal briquette resulted in more BrC being burned out. Further, far less tar balls were discovered in the images of PM_{2.5} from bio-coal briquette burning.

(3) The AAE values showed only a slight reduction compared with calculated mass-weighted average ones, which indicated that chemical species of BrC from bio-coal briquette burning has stronger wavelength dependence. The total EFs of these chemical species decrease dramatically, relatively more wavelength dependent substances are left.

In conclusion, BrC emitted from the bio-coal briquette is significantly reduced compared with calculated mass-weighted average ones. The application of bio-coal briquette technology is a promising way to control and decrease BrC emissions from residential combustion.

Supplementary Materials: The following supporting information can be downloaded at: <https://www.mdpi.com/article/10.3390/pr11061834/s1>, Table S1: The results of the orthogonal experiment of bio-coal briquette mixed with rice straw; Table S2: The results of the orthogonal experiment of bio-coal briquette mixed with corn straw; Table S3: The shatter strength analysis of rice straw-coal briquette; Table S4: The compressive strength analysis of rice straw-coal briquette; Table S5: The shatter strength analysis of corn straw-coal briquette; Table S6: The compressive strength analysis of corn straw-coal briquette.

Author Contributions: Conceptualization, J.W.; data curation, J.Q.; formal analysis, J.Q.; funding acquisition, J.W.; investigation, J.Q.; methodology, J.Q. and J.W.; project administration, J.W.; resources, J.Q. and J.W.; software, J.Q.; supervision, J.Q. and J.W.; validation, J.W.; visualization, J.W.; writing—original draft, J.Q.; writing—review and editing J.W. All authors have read and agreed to the published version of the manuscript.

Funding: This work was founded by the National Natural Science Foundation of China (No. 51974311), the Doctoral Specialty Foundation of Xuzhou College of Industrial Technology (XGY2022EA05) and the Industrial R&D projects of Xuzhou College of Industrial Technology (XGY2022CXY05).

Institutional Review Board Statement: Not applicable.

Informed Consent Statement: Not applicable.

Data Availability Statement: Not applicable.

Acknowledgments: We thank Guan, Meng from China University of Mining and Technology for her linguistic assistance during the preparation of this manuscript.

Conflicts of Interest: The authors declare no conflict of interest.

References

1. Hoffer, A.; Gelencsér, A.; Guyon, P.; Kiss, G.; Schmid, O.; Frank, G.P.; Artaxo, P.; Andreae, M.O. Optical properties of humic-like substances (HULIS) in biomass-burning aerosols. *Atmos. Chem. Phys.* **2006**, *6*, 3563–3570. [[CrossRef](#)]
2. Kirchstetter, T.W.; Novakov, T.; Hobbs, P.V. Evidence that the spectral dependence of light absorption by aerosols is affected by organic carbon. *J. Geophys. Res. Atmos.* **2004**, *109*, D21208. [[CrossRef](#)]
3. Sun, J.; Xie, C.; Xu, W.; Chen, C.; Sun, Y. Light absorption of black carbon and brown carbon in winter in North China Plain: Comparisons between urban and rural sites. *Sci. Total Environ.* **2021**, *770*, 144821. [[CrossRef](#)] [[PubMed](#)]
4. Jo, D.S.; Park, R.J.; Lee, S.; Kim, S.W.; Zhang, X. A global simulation of brown carbon: Implications for photochemistry and direct radiative effect. *Atmos. Chem. Phys.* **2016**, *15*, 27805–27852. [[CrossRef](#)]
5. Kirchstetter, T.W.; Thatcher, T.L. Contribution of organic carbon to wood smoke particulate matter absorption of solar radiation. *Atmos. Chem. Phys.* **2012**, *12*, 6067–6072. [[CrossRef](#)]
6. Feng, Y.; Ramanathan, V.; Kotamarthi, V.R. Brown carbon: A significant atmospheric absorber of solar radiation? *Atmos. Chem. Phys.* **2013**, *13*, 8607–8621. [[CrossRef](#)]
7. Wang, L.; Wang, X.; Gu, R.; Hao, W.; Wang, W. Observations of fine particulate nitrated phenols in four sites in northern China: Concentrations, source apportionment, and secondary formation. *Atmos. Chem. Phys.* **2018**, *18*, 4349–4359. [[CrossRef](#)]
8. Teich, M.; Pinxteren, D.V.; Wang, M.; Kecorius, S.; Wang, Z.; Müller, T.; Mocnik, G.; Herrmann, H. Contributions of nitrated aromatic compounds to the light absorption of water-soluble and particulate brown carbon in different atmospheric environments in Germany and China. *Atmos. Chem. Phys.* **2017**, *17*, 1653–1672. [[CrossRef](#)]
9. Li, M.; Wang, X.; Lu, C.; Li, R.; Zhang, J.; Dong, S.; Yang, L.; Xue, L.; Chen, J.; Wang, W. Nitrated phenols and the phenolic precursors in the atmosphere in urban Jinan, China. *Sci. Total Environ.* **2020**, *714*, 136760. [[CrossRef](#)]
10. Shrivastava, M.; Lou, S.; Zelenyuk, A.; Easter, R.C.; Corley, R.A.; Thrall, B.D.; Rasch, P.J.; Fast, J.D.; Massey Simonich, S.L.; Shen, H. Global long-range transport and lung cancer risk from polycyclic aromatic hydrocarbons shielded by coatings of organic aerosol. *Proc. Natl. Acad. Sci. USA* **2017**, *114*, 1246. [[CrossRef](#)]
11. Harmon, A.; Hebert, V.; Cormier, S.; Subramanian, B.; Reed, J.; Backes, W.; Dugas, T. Particulate matter containing environmentally persistent free radicals induces AhR-dependent cytokine and reactive oxygen species production in human bronchial epithelial cells. *PLoS ONE* **2018**, *13*, e0205412. [[CrossRef](#)]
12. Lu, C.; Wang, X.; Dong, S.; Zhang, J.; Li, J.; Zhao, Y.; Liang, Y.; Xue, L.; Xie, H.; Zhang, Q.; et al. Emissions of fine particulate nitrated phenols from various on-road vehicles in China. *Environ. Res.* **2019**, *179*, 108709. [[CrossRef](#)]
13. Yan, C.; Zheng, M.; Bosch, C.; Andersson, A.; Desyaterik, Y.; Sullivan, A.P.; Collett, J.L.; Zhao, B.; Wang, S.; He, K. Important fossil source contribution to brown carbon in Beijing during winter. *Sci. Rep.* **2017**, *7*, 43182. [[CrossRef](#)]
14. Gelencsér, A.; Hoffer, A.; Kiss, G.; Tombácz, E.; Bencze, L. In-situ Formation of Light-Absorbing Organic Matter in Cloud Water. *J. Atmos. Chem.* **2003**, *45*, 25–33. [[CrossRef](#)]
15. Phillips, S.M.; Smith, G.D. Light Absorption by Charge Transfer Complexes in Brown Carbon Aerosols. *Environ. Sci. Technol. Lett.* **2014**, *1*, 382–386. [[CrossRef](#)]
16. Lin, P.; Aiona, P.K.; Li, Y.; Shiraiwa, M.; Laskin, J.; Nizkorodov, S.A.; Laskin, A. Molecular Characterization of Brown Carbon in Biomass Burning Aerosol Particles. *Environ. Sci. Technol.* **2016**, *50*, 11815–11824. [[CrossRef](#)]
17. Martinsson, J.; Eriksson, A.C.; Nielsen, I.E.; Malmberg, V.B.; Ahlberg, E.; Andersen, C.; Lindgren, R.; Nyström, R.; Nordin, E.Z.; Brune, W.H.; et al. Impacts of Combustion Conditions and Photochemical Processing on the Light Absorption of Biomass Combustion Aerosol. *Environ. Sci. Technol.* **2015**, *49*, 14663–14671. [[CrossRef](#)] [[PubMed](#)]
18. Chakrabarty, R.K.; Arnold, I.J.; Francisco, D.M.; Hatchett, B.; Hosseinpour, F.; Loria, M.; Pokharel, A.; Woody, B.M. Black and brown carbon fractal aggregates from combustion of two fuels widely used in Asian rituals. *J. Quant. Spectros. Radiat. Transf.* **2013**, *122*, 25–30. [[CrossRef](#)]
19. Yan, C.; Zheng, M.; Sullivan, A.P.; Bosch, C.; Desyaterik, Y.; Andersson, A.; Li, X.; Guo, X.; Zhou, T.; Gustafsson, O. Chemical characteristics and light-absorbing property of water-soluble organic carbon in Beijing: Biomass burning contributions. *Atmos. Environ.* **2015**, *121*, 4–12. [[CrossRef](#)]
20. Mcmeeking, G.R.; Fortner, E.; Onasch, T.B.; Taylor, J.W.; Flynn, M.; Coe, H.; Kreidenweis, S.M. Impacts of nonrefractory material on light absorption by aerosols emitted from biomass burning. *J. Geophys. Res. Atmos.* **2015**, *119*, 272–286. [[CrossRef](#)]
21. Pokhrel, R.; Wagner, N.; Langridge, J.; Lack, D.; Jayarathne, T.; Stone, E.; Stockwell, C.; Yokelson, R.; Murphy, S. Parameterization of single-scattering albedo (SSA) and absorption Ångström exponent (AAE) with EC/OC for aerosol emissions from biomass burning. *Atmos. Chem. Phys.* **2016**, *16*, 9549–9561. [[CrossRef](#)]
22. Tian, J.; Wang, Q.; Ni, H.; Wang, M.; Zhou, Y.; Han, Y.; Shen, Z.; Pongpiachan, S.; Zhang, N.; Zhao, Z.; et al. Emission Characteristics of Primary Brown Carbon Absorption from Biomass and Coal Burning: Development of an Optical Emission Inventory for China. *J. Geophys. Res. Atmos.* **2019**, *124*, 1879–1893. [[CrossRef](#)]
23. Huang, R.-J.; Yang, L.; Shen, J.; Yuan, W.; Gong, Y.; Guo, J.; Cao, W.; Duan, J.; Ni, H.; Zhu, C.; et al. Water-Insoluble Organics Dominate Brown Carbon in Wintertime Urban Aerosol of China: Chemical Characteristics and Optical Properties. *Environ. Sci. Technol.* **2020**, *54*, 7836–7847. [[CrossRef](#)]
24. Voliotis, A.; Prokes, R.; Lammel, G.; Samara, C. New insights on humic-like substances associated with wintertime urban aerosols from central and southern Europe: Size-resolved chemical characterization and optical properties. *Atmos. Environ.* **2017**, *166*, 286–299. [[CrossRef](#)]

25. Krivácsy, Z.; Kiss, G.; Varga, B.; Galambos, I.; Sárvári, Z.; Gelencsér, A.; Molnár, Á.; Fuzzi, S.; Facchini, M.C.; Zappoli, S. Study of humic-like substances in fog and interstitial aerosol by size-exclusion chromatography and capillary electrophoresis. *Atmos. Environ.* **2000**, *34*, 4273–4281. [[CrossRef](#)]
26. Andreae, M.O.; Gelencsér, A. Black carbon or brown carbon? The nature of light-absorbing carbonaceous aerosols. *Atmos. Chem. Phys.* **2006**, *6*, 3131–3148. [[CrossRef](#)]
27. Chen, Y.; Bond, T.C. Light absorption by organic carbon from wood combustion. *Atmos. Chem. Phys.* **2009**, *10*, 1773–1787. [[CrossRef](#)]
28. Lin, P.; Fleming, L.T.; Nizkorodov, S.A.; Laskin, J.; Laskin, A. Comprehensive Molecular Characterization of Atmospheric Brown Carbon by High Resolution Mass Spectrometry with Electrospray and Atmospheric Pressure Photoionization. *Anal. Chem.* **2018**, *90*, 12493–12502. [[CrossRef](#)]
29. Zhang, X.; Lin, Y.H.; Surratt, J.D.; Weber, R.J. Sources, Composition and Absorption ngstrm Exponent of Light-absorbing Organic Components in Aerosol Extracts from the Los Angeles Basin. *Environ. Sci. Technol.* **2013**, *47*, 3685–3693. [[CrossRef](#)]
30. Tang, J.; Li, J.; Su, T.; Han, Y.; Mo, Y.; Jiang, H.; Cui, M.; Jiang, B.; Chen, Y.; Tang, J.; et al. Molecular compositions and optical properties of dissolved brown carbon in biomass burning, coal combustion, and vehicle emission aerosols illuminated by excitation–emission matrix spectroscopy and Fourier transform ion cyclotron resonance mass spectrometry analysis. *Atmos. Chem. Phys.* **2020**, *20*, 2513–2532.
31. Jiang, H.; Frie, A.L.; Lavi, A.; Chen, J.Y.; Zhang, H.; Bahreini, R.; Lin, Y.-H. Brown Carbon Formation from Nighttime Chemistry of Unsaturated Heterocyclic Volatile Organic Compounds. *Environ. Sci. Technol. Lett.* **2019**, *6*, 184–190. [[CrossRef](#)]
32. Liu, J.; Bergin, M.; Guo, H.; King, L.; Weber, R.J. Size-resolved measurements of brown carbon in water and methanol extracts and estimates of their contribution to ambient fine-particle light absorption. *Atmos. Chem. Phys.* **2013**, *13*, 18233–18276. [[CrossRef](#)]
33. Chakrabarty, R.K.; Moosmüller, H.; Chen, L.; Lewis, K.; Arnott, W.P.; Mazzoleni, C.; Dubey, M.K.; Wold, C.E.; Hao, W.M.; Kreidenweis, S.M. Brown carbon in tar balls from smoldering biomass combustion. *Atmos. Chem. Phys.* **2010**, *10*, 6363–6370. [[CrossRef](#)]
34. Li, C.; He, Q.; Schade, J.; Passig, J.; Zimmermann, R.; Meidan, D.; Laskin, A.; Rudich, Y. Dynamic changes in optical and chemical properties of tar ball aerosols by atmospheric photochemical aging. *Atmos. Chem. Phys.* **2019**, *19*, 139–163. [[CrossRef](#)]
35. Qi, J.; Li, Q.; Wu, J.; Jiang, J.; Miao, Z.; Li, D. Biocoal Briquettes Combusted in a Household Cooking Stove: Improved Thermal Efficiencies and Reduced Pollutant Emissions. *Environ. Sci. Technol.* **2017**, *51*, 1886–1892. [[CrossRef](#)]
36. Qi, J.; Wu, J.; Zhang, L. Influence of Molding Technology on Thermal Efficiencies and Pollutant Emissions from Household Solid Fuel Combustion during Cooking Activities in Chinese Rural Areas. *Symmetry* **2021**, *13*, 2223. [[CrossRef](#)]
37. Ikelle, I.; Eze, O. Study on the Combustion Properties of Bio-Coal Briquette Blends of Cassava Stalk. *ChemSearch J.* **2017**, *8*, 29–34.
38. Balraj, A.; Krishnan, J.; Selvarajan, K.; Sukumar, K. Potential use of biomass and coal-fine waste for making briquette for sustainable energy and environment. *Environ. Sci. Technol.* **2021**, *28*, 63516–63522. [[CrossRef](#)]
39. Sun, J.; Zhi, G.; Hitznerberger, R.; Chen, Y.; Tian, C.; Zhang, Y.; Feng, Y.; Cheng, M.; Zhang, Y.; Cai, J. Emission factors and light absorption properties of brown carbon from household coal combustion in China. *Atmos. Chem. Phys.* **2017**, *17*, 4769–4780. [[CrossRef](#)]
40. Stockwell, C.E.; Jayarathne, T.; Cochrane, M.A.; Ryan, K.C.; Putra, E.I.; Saharjo, B.H.; Nurhayati, A.D.; Albar, I.; Blake, D.R.; Simpson, I.J. Field measurements of trace gases and aerosols emitted by peat fires in Central Kalimantan, Indonesia, during the 2015 El Niño. *Atmos. Chem. Phys.* **2016**, *16*, 11711–11732. [[CrossRef](#)]
41. Fan, X.J.; Cao, T.; Xu-Fang, Y.U.; Song, J.Z.; Wang, Y.; Xiao, X.; Xie, Y.; Fei-Yue, L.I. Emission characteristics and optical properties of extractable brown carbon from residential wood combustion. *China Environ. Sci.* **2019**, *39*, 3215–3224.
42. Song, S.; Wang, Y.; Wang, Y.; Wang, T.; Tan, H. The characteristics of particulate matter and optical properties of Brown carbon in air lean condition related to residential coal combustion. *Powder Technol.* **2020**, *379*, 505–514. [[CrossRef](#)]
43. Sun, J.; Zhang, Y.; Zhi, G.; Hitznerberger, R.; Wu, C. Brown carbon’s emission factors and optical characteristics in household biomass burning: Developing a novel algorithm for estimating the contribution of brown carbon. *Atmos. Chem. Phys.* **2021**, *21*, 2329–2341. [[CrossRef](#)]
44. Utry, N.; Ajtai, T.; Filep, Á.; Pintér, M.; Török, Z.; Bozóki, Z.; Szabo, G. Correlations between absorption Angström exponent (AAE) of wintertime ambient urban aerosol and its physical and chemical properties. *Atmos. Environ.* **2014**, *91*, 52–59. [[CrossRef](#)]
45. Li, X.; Chen, Y.; Bond, T.C. Light absorption of organic aerosol from pyrolysis of corn stalk. *Atmos. Environ.* **2016**, *144*, 249–256. [[CrossRef](#)]
46. Park, S.S.; Yu, J. Chemical and light absorption properties of humic-like substances from biomass burning emissions under controlled combustion experiments. *Atmos. Environ.* **2016**, *136*, 114–122. [[CrossRef](#)]
47. Wang, Q.; Wang, L.; Li, X.; Xin, J.; Liu, Z.; Sun, Y.; Liu, J.; Zhang, Y.; Du, W.; Jin, X.; et al. Emission characteristics of size distribution, chemical composition and light absorption of particles from field-scale crop residue burning in Northeast China. *Sci. Total Environ.* **2020**, *710*, 136304. [[CrossRef](#)]
48. Li, M.; Fan, X.; Zhu, M.; Zou, C.; Song, J.; Wei, S.; Jia, W.; Peng, P.A. Abundance and Light Absorption Properties of Brown Carbon Emitted from Residential Coal Combustion in China. *Environ. Sci. Technol.* **2019**, *53*, 595–603. [[CrossRef](#)]

49. Peng, L.; Laskin, J.; Nizkorodov, S.A.; Laskin, A. Revealing Brown Carbon Chromophores Produced in Reactions of Methylglyoxal with Ammonium Sulfate. *Environ. Sci. Technol.* **2015**, *49*, 14257.
50. Bluvshstein, N.; Lin, P.; Flores, J.M.; Segev, L.; Mazar, Y.; Tas, E.; Snider, G.; Weagle, C.; Brown, S.S.; Laskin, A. Broadband optical properties of biomass burning aerosol and identification of brown carbon chromophores. *J. Geophys. Res.* **2017**, *122*, 5441–5456. [[CrossRef](#)]

Disclaimer/Publisher’s Note: The statements, opinions and data contained in all publications are solely those of the individual author(s) and contributor(s) and not of MDPI and/or the editor(s). MDPI and/or the editor(s) disclaim responsibility for any injury to people or property resulting from any ideas, methods, instructions or products referred to in the content.